Nonlinear antidamping spin-orbit torque originating from intraband transport on the warped surface of a topological insulator

Yong-Long Zhou,[1] Hou-Jian Duan,[1,2,*] Yong-jia Wu,[1] Ming-Xun Deng,[1,2] Lan Wang,[3]
Dimitrie Culcer,[4] and Rui-Qiang Wang[1,2,†]

[1]*Guangdong Provincial Key Laboratory of Quantum Engineering and Quantum Materials, School of Physics and Telecommunication Engineering, South China Normal University, Guangzhou 510006, China*

[2]*Guangdong–Hong Kong Joint Laboratory of Quantum Matter, Frontier Research Institute for Physics, South China Normal University, Guangzhou 510006, China*

[3]*School of Science and ARC Centre of Excellence in Future Low-Energy Electronics Technologies, RMIT Node, RMIT University, Melbourne, Victoria 3000, Australia*

[4]*School of Physics, The University of New South Wales, Sydney, New South Wales 2052, Australia*

(Received 23 October 2021; accepted 8 February 2022; published 17 February 2022)

Motivated by recent experiments observing a large antidamping spin-orbit torque (SOT) on the surface of a three-dimensional topological insulator, we investigate the origin of the current-induced SOT beyond linear response theory. We find that a strong antidamping SOT arises from intraband transitions in the nonlinear response and does not require interband transitions as is the case in linear transport mechanisms. The joint effect of warping and an in-plane magnetization generates a nonlinear antidamping SOT which can exceed the intrinsic one by several orders of magnitude, depending on the warping parameter and the position of the Fermi energy, and exhibits a complex dependence on the azimuthal angle of the magnetization. This nonlinear SOT provides an alternative explanation of the observed giant SOT in recent experiments.

DOI: 10.1103/PhysRevB.105.075415

I. INTRODUCTION

Electrical control of magnetic systems has a strong potential for technological applications such as fast magnetic-based storage and computational devices [1]. Recent works in this fast-evolving field have demonstrated that large spin-orbit coupling in ferromagnet/heavy-metal (FM/HM) bilayers can produce strong enough spin-orbit torques (SOTs) to switch the magnetization in the overlayer. Compared with conventional spin transfer torques in ferromagnet/insulator/ferrometal biheterostructures [2,3], this SOT has a lower current and energy threshold required for magnetization switching [4,5]. In these systems, the antidampinglike (ADL) torque has the same form as the Gilbert damping term in the Landau-Lifshitz-Gilbert equation [6] but has the opposite sign and competes against Gilbert damping to switch the magnetization. Therefore a large ADL torque is of particular importance for increasing the efficiency of magnetization switching. Antidamping torques in these structures arise from either the spin Hall effect (SHE) within the bulk of heavy metals [2,7–11] or the Rashba-Edelstein effect (or the inverse spin galvanic effect) at inversion-symmetry-broken interfaces [12–15]. They may also stem from the intrinsic Berry curvature [16], without being related to a bulk SHE.

Besides heavy metals, topological insulators (TIs) [17,18], in which the intrinsic strong spin-orbit coupling is large enough to invert the band structure, are the most promising candidates towards efficient transfer of angular momentum between the charge current and the local magnetization. Recent experiments in a FM/TI layered structure reported a giant SOT [19–25] even at room temperature. Compared with FM/HM systems the current density required for magnetization switching [23–26] in FM/TI bilayers is one to two orders of magnitude smaller, and the corresponding effective spin Hall angle [22,23] is several times larger. Most experiments have confirmed that the giant SOT originates from the surface states, e.g., the charge-to-spin current conversion efficiency increases when the Fermi energy is within the TI bulk gap rather than in the bulk states [27], excluding contributions from the SHE and Rashba-Edelstein effect. In this context, understanding the origin of the large ADL-SOT in FM/TI bilayers becomes a crucial issue.

Theoretically, there have been many efforts to explain the emergence of large SOTs, especially the antidamping component, at the magnetic surfaces of topological insulators using linear response theory. Garate and Franz [28] (see also Ref. [29]) ascribed the SOTs in FM/TI bilayers to a topological magnetoelectric effect with emphasis on its dissipationless Hall current for Fermi energies in the Dirac gap. Extending it to finite Fermi energies, this dissipationless damping was also found to arise from intrinsic interband transitions [30–33]. Mahfouzi *et al.* [34] obtained an antidamping torque by considering spin-flip reflection at an interface. Nevertheless, major questions remain unanswered. Theoretically [28–33,35,36], the ADL-SOT due to the TI surface states has been expressed in the general form

*dhjphd@163.com
†wangruiqiang@m.scnu.edu.cn

$\tau_D = \tau_d m_z \mathbf{m} \times e\mathbf{E}$, where $\mathbf{m}$ is a unit magnetization vector and $\mathbf{E}$ is the electric field. This form does not explain experimental observations because, firstly, the theoretical results of ADL-SOT are quite weak and vanish if $m_z = 0$ and, secondly, the in-plane magnetization $m_{x/y}$ has no effect on the SOT strength τ_d. Nevertheless, in the recent many experiments on FM/TI bilayers [21,25], a strong angular dependence of SOTs on the azimuthal angle of $\mathbf{m}$ was widely observed even in the absence of m_z. Doubt was even raised as to whether the experimental measurement method relying on the second harmonic Hall voltage could accurately determine the SOT due to the disturbance from asymmetric magnon scattering [37].

In this paper, we propose a mechanism for the generation of the ADL-SOT in the nonlinear response regime, purely based on the topological surface states with hexagonal warping, which is strong in realistic TIs [38,39]. Our work stands in sharp contrast to existing theories, which are exclusively based on linear response. Intriguingly, we find that the nonlinear spin polarization can produce a large ADL-SOT, caused by the interplay between the warping effect and the in-plane magnetization, which is known to have strong observable features in charge transport [40–42]. This nonlinear mechanism is distinguished from previous ones, and it can qualitatively reproduce the main features of the ADL-SOT (i.e., the giant ADL-SOT and a strong angular dependence on the azimuthal angle of the magnetization) observed in experiments.

II. THEORY FOR SOT

The SOT exerted on the FM layer has the form $\tau = \frac{2J}{\hbar}\mathbf{m} \times \mathbf{S}$ with the spin polarization $\mathbf{S} = \sum_\chi \frac{d^d\mathbf{k}}{(2\pi)^d}\mathbf{s}_\chi(\mathbf{k})f(\varepsilon_\mathbf{k}^\chi)$, where J is the s-d exchange energy, the superscript d represents the dimension, and $\mathbf{s}_\chi(\mathbf{k}) = (\hbar/2)\langle\Psi_\mathbf{k}^\chi|\boldsymbol{\sigma}|\Psi_\mathbf{k}^\chi\rangle$ is the spin expectation in the χth band with eigenvector $\Psi_\mathbf{k}^\chi$ and eigenvalue $\varepsilon_\mathbf{k}^\chi$. In the absence of applied current, the distribution function $f(\varepsilon_\mathbf{k}^\chi)$ is the Fermi-Dirac distribution function $f(\varepsilon_\mathbf{k}^\chi) = f^{(0)}(\varepsilon_\mathbf{k}^\chi) = [e^{(\varepsilon_\mathbf{k}^\chi - \varepsilon_F)/k_BT} + 1]^{-1}$ with Fermi energy ε_F and temperature T, and thus $\mathbf{S}$ vanishes due to $\mathbf{s}_\chi(-\mathbf{k}) = -\mathbf{s}_\chi(\mathbf{k})$ for spin-momentum-locked surface states of TIs. When an in-plane current is applied, the spin polarization $\mathbf{S} = \mathbf{S}^{oc} + \mathbf{S}^{in}$ can arise from the two types of change. One originates from the change in the electron occupation $\delta f(\varepsilon_\mathbf{k}^\chi) = f(\varepsilon_\mathbf{k}^\chi) - f^{(0)}(\varepsilon_\mathbf{k}^\chi)$ within the band due to acceleration by an electric field, calculated by $\mathbf{S}^{oc} = \sum_\chi \frac{d^d\mathbf{k}}{(2\pi)^d}\mathbf{s}_\chi(\mathbf{k})\delta f(\varepsilon_\mathbf{k}^\chi)$. The other stems from the modification of the quasiparticle wave functions [16,43,44], $\mathbf{S}^{in} = \sum_\chi \frac{d^d\mathbf{k}}{(2\pi)^d}\delta\mathbf{s}_\chi(\mathbf{k})f(\varepsilon_\mathbf{k}^\chi)$, where $\delta\mathbf{s}_\chi(\mathbf{k}) = (\hbar/2)\mathrm{Re}\langle\Psi_\mathbf{k}^\chi|\boldsymbol{\sigma}|\delta\Psi_\mathbf{k}^\chi\rangle$ can be traced to the interband contributions in analogy to the intrinsic contribution to the anomalous Hall effect.

We first discuss $\mathbf{S}^{oc}$ by employing the single-band steady-state Boltzmann equation [45],

$$-\frac{e}{\hbar}\mathbf{E} \cdot \nabla_\mathbf{k} f(\varepsilon_\mathbf{k}^\chi) = -\frac{f(\varepsilon_\mathbf{k}^\chi) - f^{(0)}(\varepsilon_\mathbf{k}^\chi)}{\gamma(\mathbf{k})}. \quad (1)$$

Here, we use the relaxation time approximation $\gamma(\mathbf{k}) = \gamma$. Expanding $f(\varepsilon_\mathbf{k}^\chi) = f^{(0)}(\varepsilon_\mathbf{k}^\chi) + f^{(1)}(\varepsilon_\mathbf{k}^\chi) + f^{(2)}(\varepsilon_\mathbf{k}^\chi) + \cdots$ with $f^{(n)}(\varepsilon_\mathbf{k}^\chi) \propto \mathbf{E}^n$ and then substituting it into the above Boltzmann equation, one can find the recursive relations for nth-order nonequilibrium distribution function,

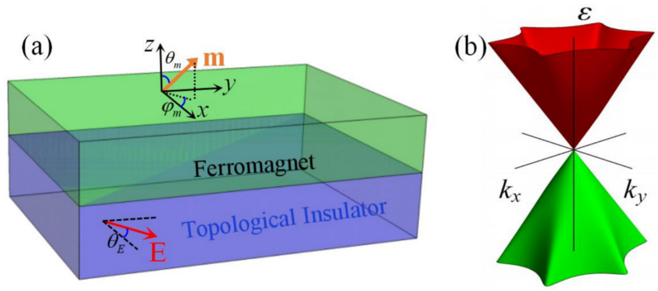

FIG. 1. (a) The FM/TI layered structure, where the orange arrow represents the local magnetic moment with magnetization $\mathbf{m}$ in the FM layer and the driven electric field $\mathbf{E} = (E_x, E_y) = |\mathbf{E}|[\cos(\theta_E), \sin(\theta_E)]$ is applied in the TI layer. (b) Schematics of the band structure for the warped surface states of TIs.

$$f^{(n)}(\varepsilon_\mathbf{k}^\chi) = \frac{e\gamma}{\hbar}\mathbf{E} \cdot \frac{\partial f^{(n-1)}(\varepsilon_\mathbf{k}^\chi)}{\partial \mathbf{k}}. \quad (2)$$

III. RESULTS AND DISCUSSION

A. Nonlinear SOT from intraband transitions

We take a FM/TI heterostructure, as shown in Fig. 1, as a sample system exhibiting a spin polarization in response to an applied electric field. On the surface of a three-dimensional TI, the effective Hamiltonian [46,47] reads

$$H_{\mathrm{TI}} = \hbar v_F(\sigma_x k_y - \sigma_y k_x) + \frac{\lambda}{2}(k_+^3 + k_-^3)\sigma_z + J\mathbf{m} \cdot \boldsymbol{\sigma}, \quad (3)$$

where v_F is the Fermi velocity, $\boldsymbol{\sigma} = (\sigma_x, \sigma_y, \sigma_z)$ is the vector of Pauli matrices acting on the real spin, and $k_\pm = k_x \pm ik_y$ with $\mathbf{k}$ being the wave vector. The first term is the Rashba-type spin-orbit coupling, the cubic-in-$\mathbf{k}$ term represents the hexagonal warping effect [38,39] of TIs with the warping parameter λ, and the FM layer is characterized by a local magnetization $\mathbf{m} = (m_x, m_y, m_z) = [\sin(\theta_m)\cos(\varphi_m), \sin(\theta_m)\sin(\varphi_m), \cos(\theta_m)]$. The energy dispersion of the Hamiltonian in Eq. (3) reads

$$\varepsilon_\mathbf{k}^\chi = \chi\hbar v_F\sqrt{(k_x - Jm_y/\hbar v_F)^2 + (k_y + Jm_x/\hbar v_F)^2 + \Lambda_\mathbf{k}^2}, \quad (4)$$

where $\Lambda_\mathbf{k} = [\lambda k_x(k_x^2 - 3k_y^2) + Jm_z]/(\hbar v_F)$ and $\chi = \pm$ are the upper and lower bands. Notice that the in-plane magnetization $m_{x/y}$ on the dispersion cannot be eliminated by performing a gauge transformation due to the existence of the warping term.

In the linear response, we retain the nonequilibrium distribution function up to the first order $f^{(1)}(\varepsilon_\mathbf{k}^\chi)$ and calculate the linear polarization $\mathbf{S}^{oc(1)} = \sum_\chi \frac{d^d\mathbf{k}}{(2\pi)^d}\mathbf{s}_\chi(\mathbf{k})f^{(1)}(\varepsilon_\mathbf{k}^\chi)$. We find that $\mathbf{S}^{oc(1)}$ only contributes to the fieldlike SOT (FL-SOT) and no antidamping SOT arises even for the case with strong warping (see Appendix A or our previous work [48]). Here, extending the theory to the nonlinear one, we calculate the nonlinear spin polarization with $\mathbf{S}^{oc(2)} = \sum_\chi \frac{d^d\mathbf{k}}{(2\pi)^d}\mathbf{s}_\chi(\mathbf{k})f^{(2)}(\varepsilon_\mathbf{k}^\chi)$. We assume that the Fermi level $\varepsilon_F > 0$ lies in the upper surface band $\chi = 1$ and the band index is suppressed afterwards. Choosing the in-plane electric field $\mathbf{E} = (E_x, E_y)$, at low temperatures we obtain the analytical expressions for the nonlinear spin polarization

$$\begin{aligned} S_x^{oc(2)} &= C\big[a_2 m_x E_y^2 + (a_1 m_z - a_2 m_y)E_x E_y\big],\\ S_y^{oc(2)} &= C\Big[\Big(\frac{a_1 m_z}{2} + a_2 m_y\Big)E_x^2 - \frac{a_1 m_z}{2}E_y^2 - a_2 m_x E_x E_y\Big],\\ S_z^{oc(2)} &= C\Big[\Big(\frac{3}{2}a_1 m_y - a_0 m_z\Big)E_x^2 - \Big(a_0 m_z + \frac{3}{2}a_1 m_y\Big)E_y^2\Big]\\ &\quad + 3Ca_1 m_x E_x E_y, \end{aligned} \tag{5}$$

where we retain up to the second-order term of $\mathbf{m}$ and λ and denote $C = e^2\gamma^2 v_F J/(8\pi)$, $a_0 = 1/(\hbar v_F \varepsilon_F)$, $a_1 = 3\lambda\varepsilon_F/(\hbar^4 v_F^4)$, and $a_2 = 3\lambda^2\varepsilon_F^3/(\hbar^7 v_F^7)$.

Interestingly, unlike the even function of $\mathbf{m}$ appearing in the linear response, the nonlinear spin polarizations in Eq. (5) are odd functions of $\mathbf{m}$ while all the second-order terms in $\mathbf{m}$ disappear. Thus the nonlinear spin polarization contributes an antidamping SOT $\tau_D^{oc} = \frac{2J}{\hbar}\mathbf{m} \times \mathbf{S}^{oc(2)}$ with strength $\tau_d^{oc} = \frac{2J}{e\hbar|\mathbf{E}|}\mathbf{S}^{oc(2)}$. The result here is significantly different from that in the linear response, where the change in the electron occupation on the Fermi surface only contributes to the FL-SOT [48]. In a FM/HM or FM/TI bilayer, the existing mechanisms for the antidamping SOT include the contribution from the Berry curvature [5,16] or the electric-field-induced intrinsic interband transition [31–33,48,49] or extrinsic disorder-induced interband-coherence effects [43]. There are also some emerging new mechanisms such as interface spin currents [50], the spin anomalous Hall effect [51], nonreciprocal generation of spin current [52], the planar Hall current [53], and the magnon [54]. These mechanisms are based on the linear response theory. Here, we propose an alternative mechanism associated with the intraband transitions beyond the linear response theory.

In order to illustrate the role of the warping effect, we set $\lambda = 0$, and Eq. (5) reduces to $S_z^{oc(2)} = \frac{-e^2\gamma^2 v_F J}{8\pi} a_0 m_z |\mathbf{E}|^2$, which is controlled only by m_z and is proportional to $1/\varepsilon_F$, and the other components vanish. This implies that the linear-$\mathbf{k}$ Dirac dispersion also can give rise to a nonlinear spin polarization, which is distinct from the electric-field-induced nonlinear current [40,41] where the current $\mathbf{j}$ vanishes for $\lambda = 0$. For finite warping $\lambda \neq 0$, not only m_z but also the in-plane magnetization $m_{x/y}$ play a role. Besides modifying the magnitude of $S_z^{oc(2)}$, $m_{x/y}$ also generate extra in-plane components $S_{x/y}^{oc(2)}$. Importantly, all of warping-related components are proportional to ε_F and λ or their higher orders. We calculate the numerical result of τ_d^{oc} directly with $\mathbf{S}^{oc(2)} = \int \frac{d^2\mathbf{k}}{(2\pi)^2}\mathbf{s}(\mathbf{k})f^{(2)}(\mathbf{k})$ rather than with the analytical expressions (5) and present the numerical result of τ_d^{oc} as a function of λ in Fig. 2(a), where all parameters are within the range of realistic TI materials. Prominently, the resulting ADL-SOT τ_d^{oc} strength increases remarkably as λ or ε_F increases. Therefore, for large ε_F and λ, τ_d^{oc} can be enhanced significantly in comparison to the case of Refs. [31–33,48] in the absence of warping. Our numerical results show that the antidamping SOT calculated from $\mathbf{S}^{oc(2)}$ in Eq. (5) is of the same order of magnitude as the FL-SOT calculated from $\mathbf{S}^{oc(1)}$ in Eq. (A7) of Appendix A, thus qualitatively reproducing the experiment result of SOT. Notice that

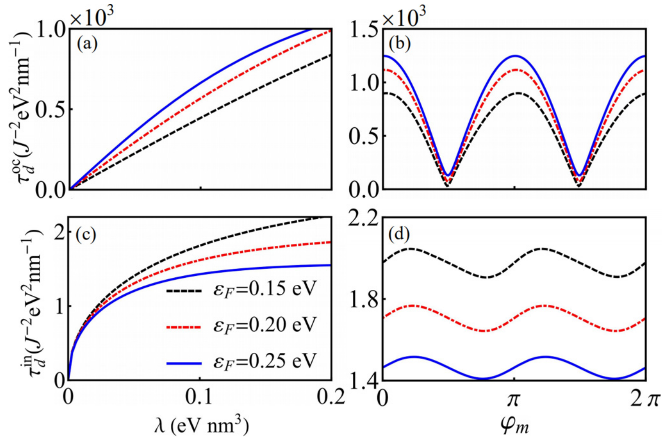

FIG. 2. Dependence of the strength of SOT (a) τ_d^{oc} and (c) τ_d^{in} on the warping parameter λ with constant azimuthal angle of $\mathbf{m}$ ($\varphi_m = \pi/4$) for different Fermi energies. (b) and (d) The φ_m -dependent strength of SOT with constant $\lambda = 0.15$ eV nm^3. Other parameters are set as follows: $\theta_m = \pi/2$, $\theta_E = \pi/4$, $v_F = 5 \times 10^5$ m/s, $\gamma = 3$ ps, and $|\mathbf{E}| = 0.2$ mV/nm.

the antidamping SOT based on the linear response theory in previous works is smaller than the FL-SOT by two to three orders of magnitude. In addition, τ_d^{oc} exhibits a complex dependence on the azimuthal angle of $\mathbf{m}$, as shown in Fig. 2(b). A complex angular dependence of the SOT has been observed in recent experimental measurements in TI bilayers [21,22,25] but has not been explained theoretically to date.

B. Understanding of intraband nonlinear damping SOT

For the linear Dirac case ($\lambda = 0$), a current-spin correspondence $\mathbf{j} = -\frac{2e}{\hbar}v_F\hat{z} \times \mathbf{S}$ can be established from the velocity operator $\hat{v} = v_F\hat{z} \times \sigma$ on the TI surface with spin-momentum locking. Here, the longitudinal conductance contributes to the FL-SOT, and the transversal conductance contributes to the dampinglike SOT. This correspondence relation is satisfied only for linear spin polarization without λ and is broken by warping [48]. For $\lambda \neq 0$, from the Hamiltonian equation (3), we can obtain the velocity operator identity

$$\hat{\mathbf{v}} = v_F(\hat{z} \times \sigma) + \frac{3\lambda k^2}{\hbar}\sigma_z[\cos(2\phi_k)\hat{x} - \sin(2\phi_k)\hat{y}], \tag{6}$$

with $\phi_k = \arctan(k_y/k_x)$. After taking the average, in the nonlinear case, the first term in the above equation vanishes, and only the second term plays a role. One cannot simply relate $\langle\sigma_z k^2\cos(2\phi_\mathbf{k})\rangle$ or $\langle\sigma_z k^2\sin(2\phi_\mathbf{k})\rangle$ to $\mathbf{S}(\mathbf{k}) = \frac{\hbar}{2}\langle\sigma_z\rangle$. Thus $\mathbf{j} \sim \mathbf{S}$ has no current-spin correspondence. Therefore we cannot simply attribute the nonlinear spin polarization to the nonlinear longitudinal or transverse conductance.

When applying an electric field on the TI surface, the hexagonal warped Fermi surface shifts in $\mathbf{k}$ space and generates a net linear spin accumulation due to the spin-momentum locking, as given by the $\mathbf{m}$-independent term in Eq. (A7) of Appendix A. However, this shift cannot generate a nonlinear spin accumulation as given in Eq. (5), where all terms are related to the magnetization $\mathbf{m}$. In order to understand the generation of the nonlinear spin polarization, we need to analyze the symmetry of the integrand in $\mathbf{S}^{oc(2)} = \int \frac{d^2\mathbf{k}}{(2\pi)^2}\mathbf{s}(\mathbf{k})f^{(2)}(\mathbf{k})$.

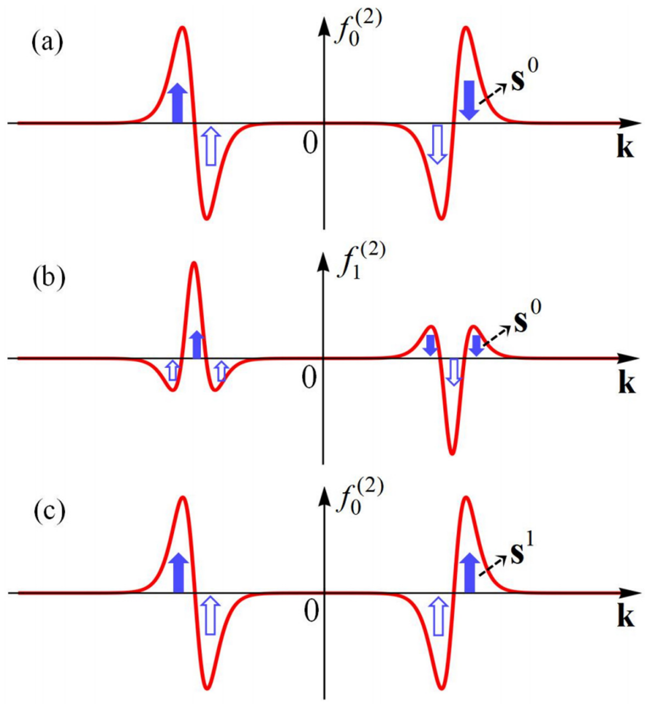

FIG. 3. Schematics of the variation of the second-order correction $f_i^{(2)}$ of the distribution function along the $\mathbf{k}$ axis parallel to the applied electric field $\mathbf{E}$. Blue solid arrows represent an excess of electrons with spins along the arrow direction, and hollow arrows represent depletion of the same. (a) describes the vanishing contribution from the component $\mathbf{s}^0(\mathbf{k})\cdot f_0^{(2)}(\mathbf{k})$. (b) and (c) The nonzero polarization stemming from the components $\mathbf{s}^0(\mathbf{k})\cdot f_1^{(2)}(\mathbf{k})$ and $\mathbf{s}^1(\mathbf{k})\cdot f_0^{(2)}(\mathbf{k})$, respectively.

In the absence of the magnetization, the average spin $\mathbf{s}(\mathbf{k})$ is odd in $\mathbf{k}$, whereas the second-order distribution function $f^{(2)}(\mathbf{k})$ is even in $\mathbf{k}$. As a consequence, $\mathbf{S}^{oc(2)}=0$. When $\mathbf{m}$ is introduced, however, the warped Fermi surface is further distorted except for the shift, which not only changes the occupation of the electron states but also perturbs the spin textures, giving an additional deviation to the spin direction at each $\mathbf{k}$ point. In this case, both $\mathbf{s}(\mathbf{k})$ and $f^{(2)}(\mathbf{k})$ have symmetric and asymmetric components with respect to $\mathbf{m}$. Up to second order in J or $\mathbf{m}$ (see Appendix C), we expand $\mathbf{s}(\mathbf{k})=\sum_{i=0,1,2}\mathbf{s}^i(\mathbf{k})J^i$ and $f^{(2)}(\mathbf{k})=\sum_{i=0,1,2}f_i^{(2)}J^i$. It is easy to check that $\mathbf{s}^i(\mathbf{k})$ is odd and $f_i^{(2)}$ is even in $\mathbf{k}$ for $i=0,2$, while $\mathbf{s}^i(\mathbf{k})$ is even and $f_i^{(2)}$ is odd for $i=1$. Thus the nonzero integrand terms of $\mathbf{k}$ in $\mathbf{S}^{oc(2)}$ are $\mathbf{s}^0(\mathbf{k})\cdot f_1^{(2)}(\mathbf{k})$ and $\mathbf{s}^1(\mathbf{k})\cdot f_0^{(2)}(\mathbf{k})$. In Fig. 3, we plot the variation of the second-order correction $f_i^{(2)}$ of the distribution function along the $\mathbf{k}$ axis parallel to the applied electric field $\mathbf{E}$. In the absence of $\mathbf{m}$ as in Fig. 3(a), the occupations of the electron states at $\mathbf{k}$ and $-\mathbf{k}$ are the same, but the corresponding spins are opposite, which contributes no net spin polarization. Once a nonzero $\mathbf{m}$ is introduced, the component $f_1^{(2)}(\mathbf{k})$ of the occupation or $\mathbf{s}^1(\mathbf{k})$ change parity. In Fig. 3(b), where both $f_1^{(2)}(\mathbf{k})$ and $\mathbf{s}^0(\mathbf{k})$ are odd, the down-spin electrons are depleted while the up-spin ones are in excess, which means that the opposite spins carried by the electrons in $\mathbf{k}$ and $-\mathbf{k}$ are unable to cancel each other, and so a net nonlinear spin polarization appears for $\mathbf{s}^0(\mathbf{k})\cdot f_1^{(2)}(\mathbf{k})$. Compared with Fig. 3(a), this is a result of $f^{(2)}(\mathbf{k})$ changing from an even to an odd function, namely, $f_0^{(2)}(\mathbf{k})\to f_1^{(2)}(\mathbf{k})$, by the interplay of the magnetization and the nontrivial spin texture of the warping effect. Figure 3(c) describes the case of $\mathbf{s}^1(\mathbf{k})\cdot f_0^{(2)}(\mathbf{k})$, where the even $f^{(2)}(\mathbf{k})$ stays the same, compared with Fig. 3(a), but $\mathbf{s}(\mathbf{k})$ is changed from an odd to an even function $\mathbf{s}^0(\mathbf{k})\to\mathbf{s}^1(\mathbf{k})$. $\mathbf{s}^1(-\mathbf{k})=\mathbf{s}^1(\mathbf{k})$ means that there are the same spin orientations at $\mathbf{k}$ and $-\mathbf{k}$, which mainly originates from the deviation of out-of-plane spin in the warping effect by the magnetization or by out-of-plane m_z. The latter contributes $S_z^{oc(2)}\propto a_0m_z$, which will quickly shrink for the Fermi energy away from the Dirac point due to $a_0\propto\frac{1}{\varepsilon_F}$. Physically, the distortion of the Fermi surface leads to a change in spin texture and an unequal population of electrons with opposite momenta as well as spins [55,56] and so generates the nonlinear spin polarization. The increasing parameter λ will enhance the distortion effect and then the nonlinear spin polarization.

C. Comparison of nonlinear SOT with intrinsic SOT

It is interesting to compare the nonlinear antidamping SOT with that from the Berry curvature caused by intrinsic interband transitions, $\mathbf{S}^{in}=\sum_\chi\frac{d^d\mathbf{k}}{(2\pi)^d}\delta\mathbf{s}_\chi(\mathbf{k})f(\varepsilon_\mathbf{k}^\chi)$, where $\delta\mathbf{s}_\chi(\mathbf{k})=(\hbar/2)\mathrm{Re}\langle\Psi_\mathbf{k}^\chi\boldsymbol{\sigma}|\delta\Psi_\mathbf{k}^\chi\rangle$. By modifying the quasiparticle wave functions $|\delta\Psi_\mathbf{k}^\chi\rangle$ with the perturbation method, the spin polarization is given by [16,43,44]

$$\mathbf{S}^{in}=\frac{e\hbar^2}{2V}\sum_{\chi\neq\chi',\mathbf{k}}\left[f\left(\varepsilon_\mathbf{k}^\chi\right)-f\left(\varepsilon_\mathbf{k}^{\chi'}\right)\right]\times\frac{\mathrm{Im}\left[\left\langle\Psi_\mathbf{k}^\chi\middle|\sigma\middle|\Psi_\mathbf{k}^{\chi'}\right\rangle\left\langle\Psi_\mathbf{k}^{\chi'}\middle|\hat{\mathbf{v}}\cdot\mathbf{E}\middle|\Psi_\mathbf{k}^\chi\right\rangle\right]}{\left(\varepsilon_\mathbf{k}^\chi-\varepsilon_\mathbf{k}^{\chi'}\right)^2}. \quad (7)$$

This expression is analogous to the intrinsic Berry-curvature mechanism originally introduced to explain the anomalous Hall effect [57] and the SHE [58] due to the electric-field-induced interband coherence. It is found that this antidamping Berry-curvature SOT can contribute with a strength comparable to that of the SHE-driven antidamping torque, and this has given a good explanation for ADL-SOT experiments with Rashba-model ferromagnets [16].

Here, we apply this intrinsic Berry-curvature mechanism to the FM/TI bilayer. For $\lambda=0$, we obtain $S_z^{in}=0$ and

$$S_{x/y}^{in}=\frac{e\hbar J}{8\pi}a_0m_zE_{x/y}. \quad (8)$$

Obviously, only m_z contributes to the spin polarization and, in turn, the intrinsic damping SOT, which recalls the results of Refs. [28,30–33,35] based on the Green's function Kubo formula. For $\lambda\neq0$, $m_{x/y}$ also play a role for the intrinsic damping. In view of the complex analytical expressions we only present the numerical results $\tau_d^{in}=\frac{2J}{e\hbar|\mathbf{E}|}|\mathbf{S}^{in}|$ in Figs. 2(c) and 2(d). Notice that in numerical calculations, we only adopt the linear part of $\mathbf{S}^{in}$ in $\mathbf{E}$. This is because the nonlinear component of $\mathbf{S}^{in}$ is an even function of $\mathbf{m}$, which only contributes the FL-SOT (see Appendix D). Physically, Eq. (7) arises from the electric-field-induced interband-virtual-transition correction. If $\delta\mathbf{s}_\chi(\mathbf{k})$ is kept up to order E^2, we have to take

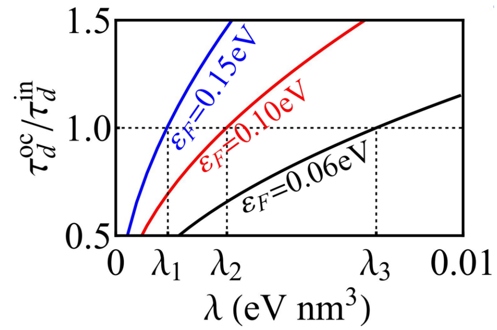

FIG. 4. The ratio τ_d^{oc}/τ_d^{in} vs the warping parameter λ. The turning points $\lambda_c = \lambda_{1\text{–}3}$ are determined by $\tau_d^{oc}/\tau_d^{in} = 1$ for different ε_F. We chose $|\mathbf{E}| = 0.004$ mV/nm, and the other parameters are the same as those in Fig. 2.

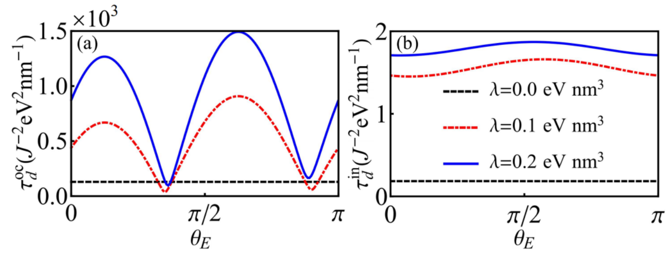

FIG. 5. The strength of SOT (a) τ_d^{oc} and (b) τ_d^{in} with respect to the current direction θ_E for different warping parameters. Parameters are set as $\varepsilon_F = 0.2$ eV, $\theta_m = 19\pi/40$, and $\varphi_m = \pi/4$. Other parameters are the same as in Fig. 2.

$\delta \mathbf{s}_\chi(\mathbf{k}) = (\hbar/2)\mathrm{Re}\langle \delta\Psi_\mathbf{k}^\chi|\boldsymbol{\sigma}|\delta\Psi_\mathbf{k}^\chi\rangle$, which is formed from the two-order interband-virtual-transition correction and usually is much smaller than the first-order one [44], and so here we will ignore this high-order term. We compare the nonlinear SOT strength τ_d^{oc} in Figs. 2(a) and 2(b) to the Berry-curvature SOT strength τ_d^{in} in Figs. 2(c) and 2(d). One can find that (i) while τ_d^{in} slightly increases with the warping parameter λ, τ_d^{oc} increases quickly; and (ii) as ε_F increases, τ_d^{oc} increases while τ_d^{in} decreases. Thus Fig. 2 shows that τ_d^{oc} is larger than τ_d^{in} by two to three orders of magnitude for the chosen parameters, which are in the range of realistic materials. In practice, the applied electric field strength in FM/TI SOT experiments [23–25] is estimated as $|\mathbf{E}| = 0.1$–0.3 mV/nm, the relaxation time in the TI Bi_2Se_3 is typically [59] $\gamma = 3$ ps, and the warping parameter [41,60] is $\lambda = 0.056$–0.18 eV nm^3. In addition, compared with τ_d^{in}, τ_d^{oc} shows a more complicated angular dependence on $\mathbf{m}$ [compare Fig. 2(b) with Fig. 2(d)].

For the case of a weak warping effect (small λ), the interband terms will become dominant. There exists a turning point λ_c determined by $\tau_d^{oc}/\tau_d^{in} = 1$. Below λ_c the linear SOT dominates, but the nonlinear SOT dominates above the turning point. The threshold λ_c of the turning point is sensitive to the Fermi energy ε_F, as depicted in Fig. 4, where different thresholds $\lambda_{1\text{–}3}$ are given for different Fermi energies. Obviously, with the increase in ε_F, the role of the warping structure in the energy band becomes more important, and the threshold of λ_c required for the nonlinear SOT τ_d^{oc} to dominate over the linear SOT τ_d^{in} becomes smaller.

Owing to the warping effect, the current-induced SOT depends on the current direction. In order to clarify the current-induced anisotropy of the SOT, we plot τ_d^{oc} and τ_d^{in} as a function of the direction of the electric field θ_E in Figs. 5(a) and 5(b), respectively. Obviously, the ADL-SOTs are isotropic for $\lambda = 0$ and anisotropic for $\lambda \neq 0$; the larger the warping parameter (or Fermi energy), the more obvious the anisotropy is. More importantly, the periods of these two kinds of SOTs are significantly different, which could lead to an enhanced ratio τ_d^{oc}/τ_d^{in} for a certain current direction θ_E.

IV. CONCLUSIONS

We have studied the current-induced nonlinear spin polarization and SOT in a FM/TI bilayer with hexagonal warping. We focus on the single-band case by employing the Boltzmann equation and find that the nonlinear spin polarization associated with intraband transitions generates a strong ADL-SOT, unlike the spin polarization linear in the electric field, which only contributes to the FL-SOT. The nonlinear antidamping SOT stems not only from the out-of-plane magnetization m_z, but also from the joint effect of warping and in-plane magnetizations m_x and m_y. The present mechanism is associated with intraband transitions, distinguished from the existing linear response theory [5,16,31–33,43,48,49], where interband transitions are necessary. More importantly, the nonlinear ADL-SOT is enhanced with increasing Fermi energy and warping parameter and can be several orders of magnitude larger than that of the intrinsic Berry-curvature contributions. It exhibits a complex dependence on the azimuthal angle of the magnetization, which is consistent with experiment. This nonlinear SOT provides a mechanism with which to explain the giant SOT in recent experiments.

ACKNOWLEDGMENTS

This work was supported by GDUPS (2017), by the National Natural Science Foundation of China (Grants No. 12174121, No. 11904107, No. 12104167, and No. 12047521), by the Guangdong NSF of China (Grants No. 2021A1515010369 and No. 2020A1515011566), by Guangdong Basic and Applied Basic Research Foundation (Grant No. 2020A1515111035). D.C. is supported by Australian Research Council Future Fellowship No. FT190100062. L.W. is supported by Australian Research Council Centre of Excellence in Future Low-Energy Electronics Technologies Award No. CE170100039.

APPENDIX A: DERIVATION OF THE LINEAR SPIN POLARIZATION

The nth-order nonequilibrium distribution function derived from Eq. (2) of the main text can be rewritten as

$$f^{(1)}(\varepsilon_\mathbf{k}^\chi) = e\gamma \mathbf{E}\cdot\mathbf{v}\frac{\partial f^{(0)}(\varepsilon_\mathbf{k}^\chi)}{\partial \varepsilon_\mathbf{k}^\chi}, \tag{A1}$$

$$f^{(2)}\left(\varepsilon_{\mathbf{k}}^{\chi}\right)=\frac{e^2\gamma^2}{\hbar}\left[\mathbf{E}\cdot\frac{\partial(\mathbf{E}\cdot\mathbf{v})}{\partial\mathbf{k}}\frac{\partial f^{(0)}\left(\varepsilon_{\mathbf{k}}^{\chi}\right)}{\partial\varepsilon_{\mathbf{k}}^{\chi}}+\hbar(\mathbf{E}\cdot\mathbf{v})^2\frac{\partial^2 f^{(0)}\left(\varepsilon_{\mathbf{k}}^{\chi}\right)}{\partial\left(\varepsilon_{\mathbf{k}}^{\chi}\right)^2}\right], \tag{A2}$$

where $\mathbf{v}=\frac{1}{\hbar}\partial_{\mathbf{k}}\varepsilon_{\mathbf{k}}^{\chi}$ is the group velocity of electrons and an in-plane electric field $\mathbf{E}=(E_x,E_y)$ is applied. For convenience, we choose a positive Fermi energy (i.e., $\varepsilon_F>0$ lies in the upper band $\chi=1$). According to the eigenvalues $\varepsilon_{\mathbf{k}}^{\chi}$ shown in Eq. (4) of the main text, the group velocity $\mathbf{v}=(v_x,v_y)$ can be easily solved as

$$\begin{aligned}v_x&=\frac{1}{\hbar\varepsilon_{\mathbf{k}}^{+}}\left[\hbar v_F(\hbar v_F k_x-Jm_y)+3\lambda\left(k_x^2-k_y^2\right)\Lambda_{\mathbf{k}}\right],\\ v_y&=\frac{1}{\hbar\varepsilon_{\mathbf{k}}^{+}}[\hbar v_F(\hbar v_F k_y+Jm_x)-6\lambda k_x k_y\Lambda_{\mathbf{k}}].\end{aligned} \tag{A3}$$

One can calculate the spin polarization using the following formula:

$$\mathbf{S}^{oc}=\sum_{\chi}\frac{d^d\mathbf{k}}{(2\pi)^d}\mathbf{s}_{\chi}(\mathbf{k})\delta f\left(\varepsilon_{\mathbf{k}}^{\chi}\right), \tag{A4}$$

where $\delta f(\varepsilon_{\mathbf{k}}^{\chi})=f(\varepsilon_{\mathbf{k}}^{\chi})-f^{(0)}(\varepsilon_{\mathbf{k}}^{\chi})$ and $\mathbf{s}_{\chi}(\mathbf{k})=(\hbar/2)\langle\Psi_{\mathbf{k}}^{\chi}|\boldsymbol{\sigma}|\Psi_{\mathbf{k}}^{\chi}\rangle$ is the spin expectation. Diagonalizing the Hamiltonian of Eq. (3) of the main text, the corresponding eigenstates can be solved as

$$\begin{aligned}|\Psi_{\mathbf{k}}^{+}\rangle&=[\cos(\xi/2),e^{i\eta}\sin(\xi/2)]^T,\\ |\Psi_{\mathbf{k}}^{-}\rangle&=[-\sin(\xi/2),e^{i\eta}\cos(\xi/2)]^T,\end{aligned} \tag{A5}$$

with $\cos(\xi)=\Lambda_{\mathbf{k}}/\varepsilon_{\mathbf{k}}^{+}$ and $\tan(\eta)=(Jm_y-\hbar v_F k_x)/(Jm_x+\hbar v_F k_y)$. Using the above eigenstates, one can calculate the spin expectation $\mathbf{s}_{+}(\mathbf{k})=(s_x,s_y,s_z)$ as

$$\mathbf{s}_{+}(\mathbf{k})=\left(\frac{J\hbar m_x+\hbar^2 v_F k_y}{2\varepsilon_{\mathbf{k}}^{+}},\frac{J\hbar m_y-\hbar^2 v_F k_x}{2\varepsilon_{\mathbf{k}}^{+}},\frac{\hbar\lambda k_x^3-3\hbar\lambda k_x k_y^2+\hbar J m_z}{2\varepsilon_{\mathbf{k}}^{+}}\right). \tag{A6}$$

Substituting Eqs. (A1) and (A6) into the spin polarization $\mathbf{S}^{oc}$ of Eq. (A4) and expanding the integrand of Eq. (A4) to the second-order term of $\mathbf{m}$ and λ, one can obtain the results for the linear spin polarization $\mathbf{S}^{oc(1)}$, which read

$$\begin{aligned}S_x^{oc(1)}&=\frac{e\gamma}{8\pi}\left[\frac{\varepsilon_F}{\hbar v_F}-\frac{1}{6}a_2\varepsilon_F^2-a_0J^2m_z^2-\frac{3}{2}a_2J^2\left(m_x^2+m_y^2-m_z^2\right)\right]E_y,\\ S_y^{oc(1)}&=\frac{e\gamma}{8\pi}\left[-\frac{\varepsilon_F}{\hbar v_F}+\frac{1}{6}a_2\varepsilon_F^2+a_0J^2m_z^2+\frac{3}{2}a_2J^2\left(m_x^2+m_y^2-m_z^2\right)\right]E_x,\\ S_z^{oc(1)}&=\frac{e\gamma J^2}{8\pi}\left\{\left[a_1\left(-m_x^2+m_y^2\right)-3a_2m_ym_z\right]E_x+(2a_1m_xm_y+3a_2m_xm_z)E_y\right\},\end{aligned} \tag{A7}$$

where $a_0=1/(\hbar v_F\varepsilon_F)$, $a_1=3\lambda\varepsilon_F/(\hbar^4v_F^4)$, and $a_2=3\lambda^2\varepsilon_F^3/(\hbar^7v_F^7)$. As shown above, all components of the linear spin polarization are even functions of $\mathbf{m}$. Thus the linear spin polarization $\mathbf{S}^{oc(1)}$ only contributes to the fieldlike SOT.

APPENDIX B: DERIVATION OF THE NONLINEAR CURRENT

For a positive Fermi energy, the charge current density can be calculated by

$$\mathbf{j}=-e\int\frac{d^d\mathbf{k}}{(2\pi)^d}\mathbf{v}_k f(\varepsilon_{\mathbf{k}}^{+}). \tag{B1}$$

Considering the linear response theory, i.e., substituting Eqs. (A1) and (A3) into the above equation, the linear current density $\mathbf{j}^{(1)}$ in FM/TI can be easily solved after some algebraic calculations. The resulting $\mathbf{j}^{(1)}$ reads as

$$\mathbf{j}^{(1)}=\sigma_D\mathbf{E}=\frac{e^2\gamma\varepsilon_F}{4\pi\hbar^2}\mathbf{E}. \tag{B2}$$

For the nonlinear response, one can substitute the nonequilibrium distribution function $f_{k,\chi}^{(2)}$ of Eq. (A2) into Eq. (B1). Following similar algebraic calculations, the nonlinear current density $\mathbf{j}^{(2)}=(j_x^{(2)},j_y^{(2)})$ can be obtained:

$$\begin{aligned}j_x^{(2)}&=c_1\left(2m_xE_xE_y-3m_yE_x^2-m_yE_y^2\right)-c_2m_z\left(E_x^2-E_y^2\right),\\ j_y^{(2)}&=c_1\left(m_xE_x^2-2m_yE_xE_y+3m_xE_y^2\right)+2c_2m_zE_xE_y,\end{aligned} \tag{B3}$$

where $c_1=3e^3\gamma^2\lambda^2J\varepsilon_F^3/(4\pi\hbar^8v_F^5)$ and $c_2=3e^3\gamma^2\lambda J\varepsilon_F/(8\pi\hbar^5v_F^2)$. As shown above, $\mathbf{j}^{(2)}=0$ when $\lambda\to 0$.

APPENDIX C: DERIVATION OF THE NONLINEAR SPIN POLARIZATION

In this Appendix, we discuss in detail the generation of the nonlinear spin polarization. To facilitate the analysis, we need to expand $\mathbf{s}(\mathbf{k})$ and $f^{(2)}(\varepsilon_{\mathbf{k}}^{+})$ to the second-order term of $\mathbf{m}$ (or the equivalent J), i.e., $\mathbf{s}(\mathbf{k})=\sum_{i=0,1,2}\mathbf{s}^i(\mathbf{k})J^i$ and $f^{(2)}(\varepsilon_{\mathbf{k}}^{\chi})=\sum_{i=0,1,2}f_i^{(2)}(\mathbf{k})J^i$.

For convenience of discussion, we here simply set the electric field as $\mathbf{E}=(E_x,0)$. For arbitrary direction of the electric field, the case is similar. In the weak-warping limit, $\mathbf{s}^i(\mathbf{k})$ and $f_i^{(2)}(\mathbf{k})$ can be expanded to the second-order term of λ, which is enough to capture the warping effect. In this way, one can obtain the analytical expressions of $\mathbf{s}^i$ and $f_i^{(2)}$. $\mathbf{s}(\mathbf{k})$ reads as

$$\mathbf{s}^0(\mathbf{k})=\left(\frac{\hbar^2 v_F k_y}{2\varepsilon_0},\ -\frac{\hbar^2 v_F k_x}{2\varepsilon_0},\ \frac{\hbar\lambda k_x^3-3\hbar\lambda k_x k_y^2}{2\varepsilon_0}\right),$$

$$\mathbf{s}^1(\mathbf{k})=\left(\frac{\hbar\varepsilon_0 m_x-\hbar^2 v_F k_y\kappa_3}{2\varepsilon_0^2},\ \frac{\hbar\varepsilon_0 m_y+\hbar^2 v_F k_x\kappa_3}{2\varepsilon_0^2},\ \frac{\hbar\varepsilon_0 m_z-\hbar\lambda k_x^3\kappa_3+3\hbar\lambda k_x k_y^2\kappa_3}{2\varepsilon_0^2}\right),$$

$$\mathbf{s}^2(\mathbf{k})=\left[\frac{\hbar^2 v_F k_y\left(3\kappa_3^2-\mathbf{m}^2\right)-2\hbar\varepsilon_0 m_x\kappa_3}{2\varepsilon_0^3},\ \frac{-\hbar^2 v_F k_x\left(3\kappa_3^2-\mathbf{m}^2\right)+2\hbar\varepsilon_{\mathbf{0}} m_y\kappa_3}{2\varepsilon_0^3},\ \frac{\hbar\lambda\left(k_x^3-3k_x k_y^2\right)\left(3\kappa_3^2-\mathbf{m}^2\right)-2\hbar\varepsilon_0 m_z\kappa_3}{2\varepsilon_0^3}\right],$$

where $\varepsilon_0=\sqrt{\lambda^2(k_x^3-3k_xk_y^2)^2+(\hbar v_F k)^2}$ and $\kappa_3=[(k_x^3-3k_xk_y^2)\lambda m_z+\hbar v_F(k_y m_x-k_x m_y)]/\varepsilon_0$. It is found that $\mathbf{s}^{0,2}(\mathbf{k})$ is odd in $\mathbf{k}$ while $\mathbf{s}^1(\mathbf{k})$ is even.

$f_i^{(2)}$ reads as

$$f_0^{(2)}=\frac{e^2\gamma^2E_x^2}{\hbar}\left[\frac{\kappa_4-\hbar^2\kappa_5^2}{\hbar\varepsilon_0}\frac{-be^{b(\varepsilon_0-\varepsilon_F)}}{(1+e^{b(\varepsilon_0-\varepsilon_F)})^2}+\hbar\kappa_5^2\frac{b^2e^{b(\varepsilon_0-\varepsilon_F)}[e^{b(\varepsilon_0-\varepsilon_F)}-1]}{[1+e^{b(\varepsilon_0-\varepsilon_F)}]^3}\right],$$

$$\begin{aligned}
f_1^{(2)}=\frac{e^2\gamma^2E_x^2}{\hbar}\Bigg\{&\frac{3\hbar\kappa_3\kappa_5^2-\hbar\kappa_3\kappa_4-2\hbar\kappa_5\left(3\lambda\left(k_x^2-k_y^2\right)m_z-\hbar v_F m_y\right)+6\lambda k_x\varepsilon_0 m_z}{\hbar\varepsilon_0^2}\times\frac{-be^{b(\varepsilon_0-\varepsilon_F)}}{(1+e^{b(\varepsilon_0-\varepsilon_F)})^2}\\
&+\frac{\kappa_4-\hbar^2\kappa_5^2}{\hbar\varepsilon_0}\times\frac{b^2e^{b(\varepsilon_0-\varepsilon_F)}[-1+e^{b(\varepsilon_0-\varepsilon_F)}]\kappa_3}{[1+e^{b(\varepsilon_0-\varepsilon_F)}]^3}\\
&+\frac{2\kappa_5\left[3\lambda\left(k_x^2-k_y^2\right)m_z-\hbar v_F m_y\right]-2\hbar\kappa_3\kappa_5^2}{\varepsilon_0}\times\frac{b^2e^{b(\varepsilon_0-\varepsilon_F)}[e^{b(\varepsilon_0-\varepsilon_F)}-1]}{[1+e^{b(\varepsilon_0-\varepsilon_F)}]^3}\\
&-\hbar\kappa_5^2\times\frac{b^3e^{b(\varepsilon_0-\varepsilon_F)}[1-4e^{b(\varepsilon_0-\varepsilon_F)}+e^{2b(\varepsilon_0-\varepsilon_F)}]\kappa_3}{[1+e^{b(\varepsilon_0-\varepsilon_F)}]^4}\Bigg\},
\end{aligned}$$

$$\begin{aligned}
f_2^{(2)}=\frac{e^2\gamma^2E_x^2}{\hbar}\Bigg\{&\frac{3\hbar^2\left(5\kappa_3^2+\mathbf{m}^2\right)\kappa_5^2+12\hbar^2\kappa_3\kappa_5\left[3\lambda\left(k_x^2-k_y^2\right)m_z-\hbar v_F m_y\right]-2\left[3\lambda\left(k_x^2-k_y^2\right)m_z-\hbar v_F m_y\right]^2+3\kappa_3^2\kappa_4\varepsilon_0}{\hbar\varepsilon_0^3}\\
&\times\frac{-be^{b(\varepsilon_0-\varepsilon_F)}}{(1+e^{b(\varepsilon_0-\varepsilon_F)})^2}+2\frac{3\hbar\kappa_3\kappa_5^2-\hbar\kappa_3\kappa_4-2\hbar\kappa_5\left[3\lambda\left(k_x^2-k_y^2\right)m_z-\hbar v_F m_y\right]+6\lambda k_x\varepsilon_0 m_z}{\hbar\varepsilon_0^2}\times\frac{\kappa_3 b^2e^{b(\varepsilon_0-\varepsilon_F)}[-1+e^{b(\varepsilon_0-\varepsilon_F)}]}{[1+e^{b(\varepsilon_0-\varepsilon_F)}]^3}\\
&+\frac{\kappa_4-\hbar^2\kappa_5^2}{\hbar\varepsilon_0}\left[\frac{b^2e^{b(\varepsilon_0-\varepsilon_F)}[1-e^{b(\varepsilon_0-\varepsilon_F)}]\left(\kappa_3^2-\mathbf{m}^2\right)}{[1+e^{b(\varepsilon_0-\varepsilon_F)}]^3\varepsilon_0}-\frac{\kappa_3^2b^3e^{b(\varepsilon_0-\varepsilon_F)}[1-4e^{b(\varepsilon_0-\varepsilon_F)}+e^{2b(\varepsilon_0-\varepsilon_F)}]}{[1+e^{b(\varepsilon_0-\varepsilon_F)}]^4}\right]\\
&+\hbar\left[\frac{2\left(4\kappa_3^2-\mathbf{m}^2\right)\kappa_5^2}{\varepsilon_0^2}-\frac{8\kappa_3\kappa_5\left[3\lambda\left(k_x^2-k_y^2\right)m_z-\hbar v_F m_y\right]}{\hbar\varepsilon_0^2}+\frac{2\left[3\lambda\left(k_x^2-k_y^2\right)m_z-\hbar v_F m_y\right]^2}{\hbar^2\varepsilon_0^2}\right]\frac{b^2e^{b(\varepsilon_0-\varepsilon_F)}[e^{b(\varepsilon_0-\varepsilon_F)}-1]}{[1+e^{b(\varepsilon_0-\varepsilon_F)}]^3}\\
&+2\frac{2\kappa_5\left[3\lambda\left(k_x^2-k_y^2\right)m_z-\hbar v_F m_y\right]-2\hbar\kappa_3\kappa_5^2}{\varepsilon_0}\times\frac{\kappa_3b^3e^{b(\varepsilon_0-\varepsilon_F)}[1-4e^{b(\varepsilon_0-\varepsilon_F)}+e^{2b(\varepsilon_0-\varepsilon_F)}]}{[1+e^{b(\varepsilon_0-\varepsilon_F)}]^4}\\
&+\hbar\kappa_5^2\left[\frac{\kappa_3^2b^4e^{b(\varepsilon_0-\varepsilon_F)}[-1+11e^{b(\varepsilon_0-\varepsilon_F)}-11e^{2b(\varepsilon_0-\varepsilon_F)}+e^{3b(\varepsilon_0-\varepsilon_F)}]}{[1+e^{b(\varepsilon_0-\varepsilon_F)}]^5}\right.\\
&\left.+\frac{b^3e^{b(\varepsilon_0-\varepsilon_F)}[1-4e^{b(\varepsilon_0-\varepsilon_F)}+e^{2b(\varepsilon_0-\varepsilon_F)}]\left(\kappa_3^2-\mathbf{m}^2\right)}{[1+e^{b(\varepsilon_0-\varepsilon_F)}]^4\varepsilon_0}\right]\Bigg\},
\end{aligned}$$

where $\kappa_4=(15k_x^4-36k_x^2k_y^2+9k_y^4)\lambda^2+(\hbar v_F)^2$ is even in $\mathbf{k}$ and $\kappa_5=[(3k_x^5-12k_x^3k_y^2+9k_xk_y^4)\lambda^2+(\hbar v_F)^2k_x]/(\hbar\varepsilon_0)$ is odd in $\mathbf{k}$, and $b=1/(k_BT)$. It is found that $f_{0,2}^{(2)}(\mathbf{k})$ is even in $\mathbf{k}$ while $f_1^{(2)}(\mathbf{k})$ is odd in $\mathbf{k}$.

All the above results indicate that the nonzero integrand terms of $\mathbf{k}$ in $\mathbf{S}^{oc(2)}$ are $\mathbf{s}^0(\mathbf{k})\cdot f_1^{(2)}(\mathbf{k})$ and $\mathbf{s}^1(\mathbf{k})\cdot f_0^{(2)}(\mathbf{k})$.

APPENDIX D: DERIVATION OF THE NONLINEAR INTRINSIC SPIN POLARIZATION

$\mathbf{S}^{in(2)}$ only contributes the fieldlike SOT (FL-SOT), and no antidamping SOT arises. To prove this, we show the detailed derivation as follows. For simplicity, we set $\mathbf{E}=(E_x,0)$, $\varepsilon_F>0$. Then, Eq. (6) of the main text can be rewritten as

$$\mathbf{S}^{in}=\frac{e\hbar^2E_x}{V}\sum_{\mathbf{k}}[f(\varepsilon_{\mathbf{k}}^{+})-f(\varepsilon_{\mathbf{k}}^{-})]\frac{\mathrm{Im}[\langle\Psi_{\mathbf{k}}^{+}|\sigma|\Psi_{\mathbf{k}}^{-}\rangle\langle\Psi_{\mathbf{k}}^{-}|\hat{v}_x|\Psi_{\mathbf{k}}^{+}\rangle]}{(2\varepsilon_{\mathbf{k}}^{+})^2},\tag{D1}$$

where $\mathrm{Im}[\langle\Psi_{\mathbf{k}}^{+}|\sigma|\Psi_{\mathbf{k}}^{-}\rangle\langle\Psi_{\mathbf{k}}^{-}|\hat{v}_x|\Psi_{\mathbf{k}}^{+}\rangle]=-\mathrm{Im}[\langle\Psi_{\mathbf{k}}^{-}|\sigma|\Psi_{\mathbf{k}}^{+}\rangle\langle\Psi_{\mathbf{k}}^{+}|\hat{v}_x|\Psi_{\mathbf{k}}^{-}\rangle]$ with $\hat{v}_x=\partial H/(\hbar\partial k_x)$. According to Eq. (A1), one can obtain the first-order distribution function $f^{(1)}(\varepsilon_{\mathbf{k}}^{\chi})=e\gamma E_xv_x\partial f^{(0)}(\varepsilon_{\mathbf{k}}^{\chi})/\partial\varepsilon_{\mathbf{k}}^{\chi}$. Substituting $f(\varepsilon_{\mathbf{k}}^{\chi})$ with $f^{(1)}(\varepsilon_{\mathbf{k}}^{\chi})$ in the above equation, one can obtain the nonlinear intrinsic spin polarization $\mathbf{S}^{in(2)}$ as

$$\mathbf{S}^{in(2)}=\frac{e^2\hbar^2\gamma E_x^2}{V}\int_{-\infty}^{\infty}dk_x\int_{-\infty}^{\infty}dk_yv_x\left[\frac{\partial f^{(0)}(\varepsilon_{\mathbf{k}}^{+})}{\partial\varepsilon_{\mathbf{k}}^{+}}-\frac{\partial f^{(0)}(\varepsilon_{\mathbf{k}}^{-})}{\partial\varepsilon_{\mathbf{k}}^{-}}\right]\frac{\mathrm{Im}[\langle\Psi_{\mathbf{k}}^{+}|\sigma|\Psi_{\mathbf{k}}^{-}\rangle\langle\Psi_{\mathbf{k}}^{-}|\hat{v}_x|\Psi_{\mathbf{k}}^{+}\rangle]}{(2\varepsilon_{\mathbf{k}}^{+})^2},\tag{D2}$$

where $\varepsilon_{\mathbf{k}}^{\pm}=\pm\sqrt{(\hbar v_Fk_x-Jm_y)^2+(\hbar v_Fk_y+Jm_x)^2+[\lambda k_x(k_x^2-3k_y^2)+Jm_z]^2}$. According to the Hamiltonian of Eq. (3) in the main text and to Eqs. (A3) and (A5), the component $S_x^{in(2)}$ can be expressed as

$$\begin{aligned}S_x^{in(2)}&=\frac{e^2\hbar^2\gamma E_x^2}{V}\int_{-\infty}^{\infty}dk_x\int_{-\infty}^{\infty}dk_yv_x\left[\frac{\partial f^{(0)}(\varepsilon_{\mathbf{k}}^{+})}{\partial\varepsilon_{\mathbf{k}}^{+}}-\frac{\partial f^{(0)}(\varepsilon_{\mathbf{k}}^{-})}{\partial\varepsilon_{\mathbf{k}}^{-}}\right]\frac{\mathrm{Im}[\langle\Psi_{\mathbf{k}}^{+}|\sigma_x|\Psi_{\mathbf{k}}^{-}\rangle\langle\Psi_{\mathbf{k}}^{-}|\hat{v}_x|\Psi_{\mathbf{k}}^{+}\rangle]}{(2\varepsilon_{\mathbf{k}}^{+})^2}\\&=\frac{e^2\hbar^2\gamma E_x^2}{V}\int_{-\infty}^{\infty}dk_x\int_{-\infty}^{\infty}dk_y\frac{\hbar v_F(\hbar v_Fk_x-Jm_y)+3\lambda\left(k_x^2-k_y^2\right)\left[\lambda\left(k_x^3-3k_xk_y^2\right)+Jm_z\right]}{\hbar\varepsilon_{\mathbf{k}}^{+}}\\&\quad\times\left[\frac{\partial f^{(0)}(\varepsilon_{\mathbf{k}}^{+})}{\partial\varepsilon_{\mathbf{k}}^{+}}-\frac{\partial f^{(0)}(\varepsilon_{\mathbf{k}}^{-})}{\partial\varepsilon_{\mathbf{k}}^{-}}\right]\frac{1}{(2\varepsilon_{\mathbf{k}}^{+})^2}\frac{\left[\hbar v_FJm_z+2\hbar v_F\lambda k_x^3-3J\lambda\left(k_x^2-k_y^2\right)m_y\right]}{\hbar\varepsilon_{\mathbf{k}}^{+}}\\&=\int_{-\infty}^{\infty}dk_x\int_{-\infty}^{\infty}dk_yF_x(\mathbf{k},\mathbf{m}).\end{aligned}\tag{D3}$$

Similarly, one can obtain

$$\begin{aligned}S_y^{in(2)}&=\frac{e^2\hbar^2\gamma E_x^2}{V}\int_{-\infty}^{\infty}dk_x\int_{-\infty}^{\infty}dk_y\frac{\hbar v_F(\hbar v_Fk_x-Jm_y)+3\lambda\left(k_x^2-k_y^2\right)\left[\lambda\left(k_x^3-3k_xk_y^2\right)+Jm_z\right]}{\hbar\varepsilon_k}\\&\quad\times\left[\frac{\partial f^{(0)}(\varepsilon_{\mathbf{k}}^{+})}{\partial\varepsilon_{\mathbf{k}}^{+}}-\frac{\partial f^{(0)}(\varepsilon_{\mathbf{k}}^{-})}{\partial\varepsilon_{\mathbf{k}}^{-}}\right]\frac{1}{(2\varepsilon_{\mathbf{k}}^{+})^2}\frac{3\lambda\left(k_x^2-k_y^2\right)(\hbar v_Fk_y+Jm_x)}{\hbar\varepsilon_{\mathbf{k}}^{+}}\\&=\int_{-\infty}^{\infty}dk_x\int_{-\infty}^{\infty}dk_yF_y(\mathbf{k},\mathbf{m}),\\S_z^{in(2)}&=\frac{e^2\hbar^2\gamma E_x^2}{V}\int_{-\infty}^{\infty}dk_x\int_{-\infty}^{\infty}dk_y\frac{\hbar v_F(\hbar v_Fk_x-Jm_y)+3\lambda\left(k_x^2-k_y^2\right)\left[\lambda\left(k_x^3-3k_xk_y^2\right)+Jm_z\right]}{\hbar\varepsilon_k}\\&\quad\times\left[\frac{\partial f^{(0)}(\varepsilon_{\mathbf{k}}^{+})}{\partial\varepsilon_{\mathbf{k}}^{+}}-\frac{\partial f^{(0)}(\varepsilon_{\mathbf{k}}^{-})}{\partial\varepsilon_{\mathbf{k}}^{-}}\right]\frac{1}{(2\varepsilon_{\mathbf{k}}^{+})^2}\frac{v_F(\hbar v_Fk_y+Jm_x)}{\varepsilon_{\mathbf{k}}^{+}}\\&=\int_{-\infty}^{\infty}dk_x\int_{-\infty}^{\infty}dk_yF_z(\mathbf{k},\mathbf{m}).\end{aligned}\tag{D4}$$

According to the above equations, we replace $\mathbf{k}$ with $-\mathbf{k}$, and then $\int_{-\infty}^{\infty}d\mathbf{k}F_{i=x,y,z}(\mathbf{k},\mathbf{m})=\int_{-\infty}^{\infty}d\mathbf{k}F_{i=x,y,z}(-\mathbf{k},\mathbf{m})$. At the same time, all the integrands $F_i(\mathbf{k},\mathbf{m})$ in $\mathbf{S}^{in(2)}$ satisfy $F_{i=x,y,z}(-\mathbf{k},-\mathbf{m})=F_{i=x,y,z}(\mathbf{k},\mathbf{m})$. Thus one can find that $\int_{-\infty}^{\infty}d\mathbf{k}F_{i=x,y,z}(\mathbf{k},-\mathbf{m})=\int_{-\infty}^{\infty}d\mathbf{k}F_{i=x,y,z}(-\mathbf{k},-\mathbf{m})=\int_{-\infty}^{\infty}d\mathbf{k}F_{i=x,y,z}(\mathbf{k},\mathbf{m})$. This means that the results of $\mathbf{S}^{in(2)}$ are even functions of $\mathbf{m}$, which only contributes FL-SOT. Thus we do not need to consider $\mathbf{E}^2$ corrections to $\mathbf{S}^{in}$.

[1] I. Žutić, J. Fabian, and S. D. Sarma, Rev. Mod. Phys. **76**, 323 (2004).
[2] A. Manchon, J. Železný, I. M. Miron, T. Jungwirth, J. Sinova, A. Thiaville, K. Garello, and P. Gambardella, Rev. Mod. Phys. **91**, 035004 (2019).
[3] G. Prenat, K. Jabeur, G. Di Pendina, O. Boulle, and G. Gaudin, in *Spintronics-Based Computing*, edited by W. Zhao and G. Prenat (Springer, Cham, Switzerland, 2015), pp. 145–157.
[4] G. Prenat, K. Jabeur, P. Vanhauwaert, G. D. Pendina, F. Oboril, R. Bishnoi, M. Ebrahimi, N. Lamard, O. Boulle, K. Garello,

J. Langer, B. Ocker, M.-C. Cyrille, P. Gambardella, M. Tahoori, and G. Gaudin, IEEE Trans. Multi-Scale Comput. Syst. **2**, 49 (2016).
[5] K.-S. Lee, D. Go, A. Manchon, P. M. Haney, M. D. Stiles, H.-W. Lee, and K.-J. Lee, Phys. Rev. B **91**, 144401 (2015); **93**, 179901(E) (2016).
[6] T. Yokoyama, Phys. Rev. B **84**, 113407 (2011).
[7] L. Liu, C.-F. Pai, Y. Li, H. W. Tseng, D. C. Ralph, and R. A. Buhrman, Science **336**, 555 (2012).
[8] L. Liu, O. J. Lee, T. J. Gudmundsen, D. C. Ralph, and R. A. Buhrman, Phys. Rev. Lett. **109**, 096602 (2012).
[9] L. Liu, C.-F. Pai, D. C. Ralph, and R. A. Buhrman, Phys. Rev. Lett. **109**, 186602 (2012).
[10] J. Sinova, S. O. Valenzuela, J. Wunderlich, C. H. Back, and T. Jungwirth, Rev. Mod. Phys. **87**, 1213 (2015).
[11] J. Sinova and T. Jungwirth, Phys. Today **70**(7), 38 (2017).
[12] M. Trushin and J. Schliemann, Phys. Rev. B **75**, 155323 (2007).
[13] I. M. Miron, T. Moore, H. Szambolics, L. D. Buda-Prejbeanu, S. Auffret, B. Rodmacq, S. Pizzini, J. Vogel, M. Bonfim, A. Schuhl, and G. Gaudin, Nat. Mater. **10**, 419 (2011).
[14] T. D. Skinner, K. Olejník, L. K. Cunningham, H. Kurebayashi, R. P. Campion, B. L. Gallagher, T. Jungwirth, and A. J. Ferguson, Nat. Commun. **6**, 6730 (2015).
[15] L. Chen, M. Gmitra, M. Vogel, R. Islinger, M. Kronseder, D. Schuh, D. Bougeard, J. Fabian, D. Weiss, and C. H. Back, Nat. Electron. **1**, 350 (2018).
[16] H. Kurebayashi, J. Sinova, D. Fang, A. C. Irvine, T. D. Skinner, J. Wunderlich, V. Novák, R. P. Campion, B. L. Gallagher, E. K. Vehstedt, L. P. Zârbo, K. Výborný, A. J. Ferguson, and T. Jungwirth, Nat. Nanotechnol. **9**, 211 (2014).
[17] M. Z. Hasan and C. L. Kane, Rev. Mod. Phys. **82**, 3045 (2010).
[18] X.-L. Qi and S.-C. Zhang, Rev. Mod. Phys. **83**, 1057 (2011).
[19] Y. Wang, P. Deorani, K. Banerjee, N. Koirala, M. Brahlek, S. Oh, and H. Yang, Phys. Rev. Lett. **114**, 257202 (2015).
[20] Y. Fan, X. Kou, P. Upadhyaya, Q. Shao, L. Pan, M. Lang, X. Che, J. Tang, M. Montazeri, K. Murata, L.-T. Chang, M. Akyol, G. Yu, T. Nie, K. L. Wong, J. Liu, Y. Wang, Y. Tserkovnyak, and K. L. Wang, Nat. Nanotechnol. **11**, 352 (2016).
[21] A. R. Mellnik, J. S. Lee, A. Richardella, J. L. Grab, P. J. Mintun, M. H. Fischer, A. Vaezi, A. Manchon, E.-A. Kim, N. Samarth, and D. C. Ralph, Nature (London) **511**, 449 (2014).
[22] Y. Fan, P. Upadhyaya, X. Kou, M. Lang, S. Takei, Z. Wang, J. Tang, L. He, L.-T. Chang, M. Montazeri, G. Yu, W. Jiang, T. Nie, R. N. Schwartz, Y. Tserkovnyak, and K. L. Wang, Nat. Mater. **13**, 699 (2014).
[23] J. Han, A. Richardella, S. A. Siddiqui, J. Finley, N. Samarth, and L. Liu, Phys. Rev. Lett. **119**, 077702 (2017).
[24] Y. Wang, D. Zhu, Y. Wu, Y. Yang, J. Yu, R. Ramaswamy, R. Mishra, S. Shi, M. Elyasi, K.-L. Teo, Y. Wu, and H. Yang, Nat. Commun. **8**, 1364 (2017).
[25] D. C. Mahendra, R. Grassi, J.-Y. Chen, M. Jamali, D. R. Hickey, D. Zhang, Z. Zhao, H. Li, P. Quarterman, Y. Lv, M. Li, A. Manchon, K. A. Mkhoyan, T. Low, and J.-P. Wang, Nat. Mater. **17**, 800 (2018).
[26] C. H. Li, O. M. J. van't Erve, S. Rajput, L. Li, and B. T. Jonker, Nat. Commun. **7**, 13518 (2016).
[27] M. Mogi, K. Yasuda, R. Fujimura, R. Yoshimi, N. Ogawa, A. Tsukazaki, M. Kawamura, K. S. Takahashi, M. Kawasaki, and Y. Tokura, Nat. Commun. **12**, 1404 (2021).
[28] I. Garate and M. Franz, Phys. Rev. Lett. **104**, 146802 (2010).
[29] D. Kurebayashi and N. Nagaosa, Phys. Rev. B **100**, 134407 (2019).
[30] P. B. Ndiaye, C. A. Akosa, M. H. Fischer, A. Vaezi, E.-A. Kim, and A. Manchon, Phys. Rev. B **96**, 014408 (2017).
[31] T. Yokoyama, J. Zang, and N. Nagaosa, Phys. Rev. B **81**, 241410(R) (2010).
[32] T. Chiba, S. Takahashi, and G. E. W. Bauer, Phys. Rev. B **95**, 094428 (2017).
[33] A. Sakai and H. Kohno, Phys. Rev. B **89**, 165307 (2014).
[34] F. Mahfouzi, B. K. Nikolić, and N. Kioussis, Phys. Rev. B **93**, 115419 (2016).
[35] T. Chiba and T. Komine, Phys. Rev. Appl. **14**, 034031 (2020).
[36] T. Gao, A. Qaiumzadeh, H. An, A. Musha, Y. Kageyama, J. Shi, and K. Ando, Phys. Rev. Lett. **121**, 017202 (2018).
[37] K. Yasuda, A. Tsukazaki, R. Yoshimi, K. Kondou, K. S. Takahashi, Y. Otani, M. Kawasaki, and Y. Tokura, Phys. Rev. Lett. **119**, 137204 (2017).
[38] R. S. Akzyanov and A. L. Rakhmanov, Phys. Rev. B **97**, 075421 (2018).
[39] R. S. Akzyanov and A. L. Rakhmanov, Phys. Rev. B **99**, 045436 (2019).
[40] S. S.-L. Zhang and G. Vignale, in *Spintronics XI*, Proceedings of SPIE (SPIE, Bellingham, WA, 2018), Vol. 10732, p. 1073215.
[41] P. He, S. S.-L. Zhang, D. Zhu, Y. Liu, Y. Wang, J. Yu, G. Vignale, and H. Yang, Nat. Phys. **14**, 495 (2018).
[42] P. Bhalla, A. H. MacDonald, and D. Culcer, Phys. Rev. Lett. **124**, 087402 (2020).
[43] C. Xiao and Q. Niu, Phys. Rev. B **96**, 045428 (2017).
[44] I. Garate and A. H. MacDonald, Phys. Rev. B **80**, 134403 (2009).
[45] C.-X. Liu, X.-L. Qi, H. J. Zhang, X. Dai, Z. Fang, and S.-C. Zhang, Phys. Rev. B **82**, 045122 (2010).
[46] Y. L. Chen, J. G. Analytis, J.-H. Chu, Z. K. Liu, S.-K. Mo, X. L. Qi, H. J. Zhang, D. H. Lu, X. Dai, Z. Fang, S. C. Zhang, I. R. Fisher, Z. Hussain, and Z.-X. Shen, Science **325**, 178 (2009).
[47] L. Fu, Phys. Rev. Lett. **103**, 266801 (2009).
[48] J.-Y. Li, R.-Q. Wang, M.-X. Deng, and M. Yang, Phys. Rev. B **99**, 155139 (2019).
[49] H. Li, H. Gao, L. P. Zârbo, K. Výborný, X. Wang, I. Garate, F. Doğan, A. Čejchan, J. Sinova, T. Jungwirth, and A. Manchon, Phys. Rev. B **91**, 134402 (2015).
[50] V. P. Amin, J. Zemen, and M. D. Stiles, Phys. Rev. Lett. **121**, 136805 (2018).
[51] S. Iihama, T. Taniguchi, K. Yakushiji, A. Fukushima, Y. Shiota, S. Tsunegi, R. Hiramatsu, S. Yuasa, Y. Suzuki, and H. Kubota, Nat. Electron. **1**, 120 (2018).
[52] G. Okano, M. Matsuo, Y. Ohnuma, S. Maekawa, and Y. Nozaki, Phys. Rev. Lett. **122**, 217701 (2019).
[53] C. Safranski, E. A. Montoya, and I. N. Krivorotov, Nat. Nanotechnol. **14**, 27 (2019).
[54] N. Okuma and K. Nomura, Phys. Rev. B **95**, 115403 (2017).
[55] Y. H. Wang, D. Hsieh, D. Pilon, L. Fu, D. R. Gardner, Y. S. Lee, and N. Gedik, Phys. Rev. Lett. **107**, 207602 (2011).
[56] M. Nomura, S. Souma, A. Takayama, T. Sato, T. Takahashi, K. Eto, K. Segawa, and Y. Ando, Phys. Rev. B **89**, 045134 (2014).
[57] N. Nagaosa, J. Sinova, S. Onoda, A. H. MacDonald, and N. P. Ong, Rev. Mod. Phys. **82**, 1539 (2010).

[58] J. Sinova, D. Culcer, Q. Niu, N. A. Sinitsyn, T. Jungwirth, and A. H. MacDonald, Phys. Rev. Lett. **92**, 126603 (2004).

[59] Y. D. Glinka, S. Babakiray, T. A. Johnson, A. D. Bristow, M. B. Holcomb, and D. Lederman, Appl. Phys. Lett. **103**, 151903 (2013).

[60] K. Kuroda, M. Arita, K. Miyamoto, M. Ye, J. Jiang, A. Kimura, E. E. Krasovskii, E. V. Chulkov, H. Iwasawa, T. Okuda, K. Shimada, Y. Ueda, H. Namatame, and M. Taniguchi, Phys. Rev. Lett. **105**, 076802 (2010).